

Document downloaded from:

<http://hdl.handle.net/10251/88159>

This paper must be cited as:

Bas Cerdá, MDC.; Ortiz Moragón, J.; Ballesteros Pascual, L.; Martorell Alsina, SS. (2017). Forecasting 7BE concentrations in surface air using time series analysis. *Atmospheric Environment*. 155:154-161. doi:10.1016/j.atmosenv.2017.02.021.



The final publication is available at

<https://doi.org/10.1016/j.atmosenv.2017.02.021>

Copyright Elsevier

Additional Information

1 FORECASTING ⁷BE CONCENTRATIONS IN SURFACE AIR USING TIME SERIES ANALYSIS

2 María del Carmen Bas, Ph.D* , Josefina Ortiz, Luisa Ballesteros, Sebastian Martorell, Ph.D

3 *Laboratorio de Radiactividad Ambiental, Grupo MEDASEGI, Universitat Politècnica de Valencia, Spain*

5 Abstract

6 ⁷Be is a cosmogenic radionuclide widely used as an atmospheric tracer, whose evaluation and forecasting can
7 provide valuable information on changes in the atmospheric behavior. In this study, measurements of ⁷Be
8 concentrations were made each month during the period 2007-2015 from samples of atmospheric aerosols
9 filtered from the air. The aim was to propose a Seasonal Autoregressive Integrated Moving Average (SARIMA)
10 model to develop an explanatory and predictive model of ⁷Be air concentrations. The Root Mean Square Error
11 (RMSE) and the Adapted Mean Absolute Percentage Error (AMAPE) were selected to measure forecasting
12 accuracy in identifying the best historical data time window to explain ⁷Be concentrations. A measure based on
13 the variance of forecast errors was calculated to determine the impact of the model uncertainty on forecasts.
14 We concluded that the SARIMA method is a powerful explanatory and predictive technique for explaining ⁷Be
15 air concentrations in a long-term series of at least eight years of historical data to forecast ⁷Be concentration
16 trends up to one year in advance.

17

18 **Keywords:** ⁷Be, time series, Forecasting, SARIMA model.

19

20 1. Introduction

21 ⁷Be is widely used as an atmospheric radiotracer due to its relatively short life ($T_{1/2} = 53.3$ days) and ease of
22 measurement by γ -spectrometry, which provides important information on atmospheric air mass motions. A
23 better understanding of its distribution would facilitate refinement and validation of global atmospheric
24 circulation models (Dueñas et al. 2015). ⁷Be forecasting can thus be adopted as a target value in analyzing
25 fluctuations or deviations that could imply important atmospheric changes.

26 ⁷Be is a cosmogenic radionuclide formed by spallation reactions of light atmospheric nuclei (such as carbon,
27 nitrogen and oxygen) with very high-energy protons and neutrons of the primary cosmic rays (Lal et al., 1958;
28 Bruninx, 1961). Most ⁷Be production (~70%) occurs in the stratosphere and the remainder (~30%) is produced
29 in the troposphere, so that the ⁷Be production rate is altitude-dependent (Feely et al., 1989; Baeza et al., 1996;
30 Kotsopoulou & Ioannidou, 2012).

31 It is generally accepted that the ⁷Be production rate depends on a number of atmospheric factors. Several studies
32 have pointed out that the intensity of galactic cosmic rays in the Earth's orbit is affected by solar activity and
33 the geomagnetic field, which is under constant cosmic ray bombardment from space (O'Brien, 1979; Vogt et
34 al., 1990; Hötzl et al., 1991; Ioannidou & Papastefanou, 1994). In particular, an increase in solar activity and
35 geomagnetic field reduce the galactic cosmic ray flux, which is followed by reduced ⁷Be production.

36 In addition to the above-mentioned sources of variability, ⁷Be concentrations in the lower layers of the
37 atmosphere present temporal variations caused by solar radiation and meteorological parameters that can affect
38 regional weather patterns (temperature, relative humidity, precipitations, wind speed and wind direction) (Feely
39 et al., 1989; Baeza et al., 1996).

40 A recent study applied a decomposition of the ⁷Be time series into a trend-cycle, a seasonal and an irregular
41 component in order to separate the inter- and intra-annual patterns of ⁷Be variability (Bas et al, 2016). The

42 results of this study showed the need to apply time series analysis to correlated data in order to separate the
43 different sources of variability of ⁷Be concentrations and to develop a forecasting model.

44 Many research studies have applied Multiple Linear Regression (MLR) analysis to develop a forecasting model
45 for ⁷Be air concentrations using atmospheric and meteorological variables as predictors (e.g. Azahra et al,
46 2004a, 2004b; Piñero-García et al., 2012, 2013; Dueñas et al., 1999, 2015). However, the disadvantage of the
47 MLR technique is that it requires forecast meteorological parameters to predict ⁷Be air concentrations. Several
48 authors recommend the use of time series modeling techniques when monitoring correlated process data (Alwan
49 & Roberts 1988; Harris & Ross 1991; Wardell et al. 1994).

50 The objective of this study is to propose a seasonal Autoregressive Integrated Moving Average (SARIMA)
51 model to develop a powerful explanatory and forecasting model of ⁷Be air concentrations. For this, different
52 data ranges of historical data are proposed to identify and validate the number of periods which best fit to ⁷Be
53 data. The optimal range of historical data is identified by means of the Root Mean Square Error (RMSE) and
54 the Adapted Mean Absolute Percentage Error (AMAPE) as forecasting accuracy measures. The impact of the
55 model uncertainty on forecasts is measured by the variance of the forecast errors.

56

57 **2. Material and Methods**

58

59 *2.1. Study area and sampling*

60 Airborne particulate samples were collected weekly on the campus of the Universitat Politècnica de Valencia
61 from January 2007 to December 2015. Valencia is situated on the east coast of Spain (15m above sea level) in
62 the western Mediterranean Basin (39°28'50" N, 0°21'59" W) and has a relatively dry subtropical Mediterranean
63 climate with very mild winters and long hot summers. The sampling point was located approximately 2 km
64 away from the coastline.

65 Aerosol samples were collected using Eberlyne G21DX and Saic AVS28A air samplers placed approximately
66 1 m above ground level. The aerosol particles were retained on a cellulose filter of 4.2×10^{-2} m effective
67 diameter and 0.8 μ m pore size. The filters were changed weekly and the average volume ranged from 300 to
68 400 m³ per week. Each filter was put inside a plastic box and kept in a desiccator until it was measured.

69 *2.2. ⁷Be activity measurements*

70

71 A monthly composite sample containing 4-5 filters was measured by γ -spectrometry to determine specific ⁷Be
72 activities using an HPGe detector (ORTEC Industries, USA) n-type with relative efficiency of 18% for 60Co
73 gamma-ray. A certificated standard containing radionuclides with energies ranging from 59 to 1836.1 keV was
74 used for preparing the calibrated filters, which were placed inside their plastic boxes on the top of the detector.
75 The counting time was 60000s and the γ -line 477.7 KeV was used to calculate the activity. ORTEC Gamma-
76 Vision software was used for acquisition and analysis. Concentration activities were corrected for the
77 radioactive decay to the mid-collection period. The mean measured uncertainties (K=2) were around 10 %.

78

79 *2.3. Statistical analysis*

80

81 A time series is a sequence of observations taken sequentially in time and influenced by four separate
82 components: (i) a *trend component* or long-term movement, (ii) a *cycle component* or fluctuations about the
83 trend of greater or lesser regularity (iii) a *seasonal component* reflecting seasonality, and (iv) a random or
84 *irregular component*. Several techniques are available for separating the trend component from oscillating
85 fluctuations and random variations in a seasonal time series. One of the most frequently used methods for
86 estimating a time series is the method of the Seasonal Autoregressive Integrated Moving Average (SARIMA)
87 model (Box & Jenkins 1976).

88

89 The SARIMA model building process is designed to take advantage of the association in the sequentially lagged
 90 relationships that usually exist in data collected periodically. If the time series has more than one seasonal
 91 behavior, for instance two, s and s^1 , the model will be composed of more parameters in order to model the
 92 other seasonal period, e.g. SARIMA(p, d, q)(P, D, Q) $_s(P^1, D^1, Q^1)_{s^1}$.

93 According to Bas et al. (2016), ^7Be concentration variability can be decomposed in terms of three main
 94 components: 1) trend-cycle, 2) seasonal and 3) irregular variations. Therefore, in principle, two periods could
 95 be considered, i.e. trend-cycle (11 years solar cycle) and seasonal (12 months). The trend-cycle component
 96 could not be totally modeled because the evaluated period was too short (2007-2015). In order to explicitly
 97 model the three parameters P^1, D^1, Q^1 of the trend-cycle component we needed more representative sample
 98 data. However, the model was able to capture part of the trend in the data with the d parameter, as explained
 99 below. We could therefore only model one seasonal period: annual periodicity.

100 A time series $\{z_t, t = 1, \dots, N\}$ is generated by a SARIMA(p, d, q)(P, D, Q) $_s$ model for only one seasonal period
 101 if:

$$102 \quad \phi_p(B)\Phi_P(B^s)(1-B)^d(1-B^s)^D z_t = \theta_q(B)\Theta_Q(B^s)a_t \text{ (eq. 1)}$$

103 where N is the number of observations; p, d, q, P, D, Q are integers; B is the lag operator (e.g. $(1-B)z_t = z_t -$
 104 z_{t-1} ; $(1-B^{12})z_t = z_t - z_{t-12}$); s is the seasonal period length; d is the number of regular differences ($d \leq$
 105 2); D is the number of seasonal differences, and a_t is the random event or estimated residual at time t , which is
 106 a usual Gaussian white noise process (WN).
 107
 108
 109

110 $\phi_p(B) = 1 - \phi_1 B - \phi_2 B^2 - \dots - \phi_p B^p$; (eq. 2), is the regular autoregressive operator (AR) of order p ,
 111 $\theta_q(B) = 1 - \theta_1 B - \theta_2 B^2 - \dots - \theta_q B^q$; (eq. 3), is the regular moving average operator (MA) of order q ,
 112 $\Phi_P(B^s) = 1 - \Phi_1 B^s - \Phi_2 B^{s^2} - \dots - \Phi_P B^{s^P}$; (eq. 4), is the seasonal autoregressive operator (SAR) of order
 113 P ,
 114 $\Theta_Q(B^s) = 1 - \Theta_1 B^s - \Theta_2 B^{s^2} - \dots - \Theta_Q B^{s^Q}$; (eq. 5), is the seasonal moving average operator (SMA) of order
 115 Q .
 116

117 The parameters $(p, d, q)(P, D, Q)_s$ try to model the time series behavior in the period evaluated. The first part
 118 of the SARIMA defined by the (p, d, q) parameters is related to the regular part of the time series and the
 119 $(P, D, Q)_s$ with seasonal variations.
 120

121 Considering the annual periodicity observed in Bas et al. (2016) and the ^7Be values measured monthly, the
 122 parameters of the SARIMA model have the following interpretation:
 123

124 p : determines the influence of the previous months of the same year on the forecasting month. It is known as
 125 the time series inertia. p is represented by $\phi_p(B)$ in Eq.1, which is defined in Eq. 2.

126 d : associated with the influence of the trend on the time series. The parameter d represents the times that the
 127 time series should be differenced in order to eliminate the trend. d is represented by $(1-B)^d$ in Eq. 1.

128 q : determines the influence of random events produced by external factors, which affected previous months of
 129 the same year, on the forecasting month. q is represented by $\theta_q(B)$ in Eq.1, which is defined in Eq. 3.

130 P : determines the influence of the months of past years on the forecasting month. P is represented by $\Phi_P(B^s)$ in
 131 Eq.1, which is defined in Eq. 4.

132 D : associated with the influence of the seasonal behavior on the time series. The parameter D represents the
 133 times that the time series should be differenced in order to eliminate the visual part of the seasonality. If the
 134 time series has a seasonal period, it is necessary to eliminate this seasonality in order to identify real
 135 relationships between the values of the time series. D is represented by $(1-B^s)^D$ in Eq. 1.

136 Q : determines the influence of random events produced by external factors, which affected months of past
137 years, on the forecasting month. Q is represented by $\theta_Q(B^S)$ in Eq.1, which is defined in Eq. 5.

138

139 As reported by Box & Jenkins (1976) and Shumway & Stoffer (2006), the SARIMA model consists of three
140 main steps:

141 **Identification and estimation step**

142 First, the periodogram technique was applied to identify the periodic cycle in the time series (Schuster, 1898).
143 The periodogram plot should have clear peaks at points corresponding to the periodic cycle in the cyclic model.

144 The time series should then be differenced in order to be stationary in mean and variance (identifying d and D
145 parameters). Differencing is a technique that can also be used to remove trends. Trends are usually detected by
146 inspecting the plot of the ${}^7\text{Be}$ data over the period considered. However, they are also characterized by the
147 autocorrelation function.

148 After differencing the time series, a tentative autoregressive moving average (ARMA) process is carried out
149 based on the estimated autocorrelation function (ACF) and the estimated partial autocorrelation function
150 (PACF). The shape of the ACF and PACF of the real time series is compared with the shape of the theoretical
151 model to identify possible different parameters p , q , P and Q of the SARIMA model (Peña, 2010; Shumway &
152 Stoffer, 2006). Having specified tentative models in the identification step, the parameters of the candidate
153 models are estimated by a maximum likelihood function (Shine & Lee, 2000).

154 After trying several combinations for parameters p , q , P and Q , the best and most parsimonious model was
155 selected, considering the minimum AMAPE and RMSE (defined in the section on the Forecasting Step) for the
156 forecasting data as accuracy measures of the predictive power.

157 **Validation step**

158 In this step, the below statistical tests were used to check the adequacy of the identified models for each time
159 period. An essential part of the procedure is to examine the residuals of the SARIMA model, which should be
160 considered, if the model is satisfactory, as White Noise (WN). We examine some simple tests for checking
161 the hypothesis that the residuals are WN and the model is valid. If the fit model passes the following tests, it
162 can be used to make a forecast.

163

- 164 - *t-ratio test* to evaluate the significance of the parameters estimated in each model. The parameters are
165 considered significant with a 95% of confidence level if $p\text{-values} < 0.05$.
- 166 - *Kolmogorov-Smirnov (K-S) test* applying Lilliefors correction of the residual series to check that the noise
167 process is Gaussian. The residual series is Gaussian if $p\text{-values} > 0.05$.
- 168 - *Q^* Ljung-Box test* to check the condition that the residuals can be considered as a WN. The statistic
169 proposed is

$$170 \quad Q^* = n(n + 2) \sum_{k=1}^m (n - k)^{-1} r_k(a) \quad (\text{eq. 6})$$

171 where $r_k(\varepsilon)$ is the sample autocorrelation f order k of the residual, n is the length of residual series and m is
172 the number of lags considered, $Q^* \approx \chi^2_{m-n}$, $n = p + q + P + Q$. The model is considered valid if
173 $P(\chi^2(m - n) > Q^*) = p\text{-value} > 0.05$. In this study, Q^* Ljung-Box statistic is calculated for a large m in
174 each model, as suggested by Peña (2010).

175

176

177

178

179

180 Forecasting step

181 To assess the forecasting performance of different models each data set is divided into two samples for training
182 and testing. This procedure is known as an out-of-sample technique, which means that the training data used in
183 model fitting are different to the test sample (out-of-sample) used to evaluate the established model.

184

185 Several measurement statistics can be used to examine the forecast accuracy of different models. Root Mean
186 Square Error (RMSE) and Mean Absolute Percentage Error (MAPE) are the most frequently used criteria to
187 evaluate the performance of the forecasting models. One of the disadvantages of the MAPE criteria is the
188 adverse effect of small actual values, in which case MAPE criteria will contribute large terms to the MAPE
189 coefficient, even if the difference between the actual and forecast values is small. It is therefore better to use an
190 adapted MAPE (AMAPE), as defined in various studies (Tsay, 2005; Wu & Shahidehpour, 2010):

$$191 \quad RMSE = \sqrt{\frac{\sum_{t=1}^n (\hat{z}_t - z_t)^2}{n}} \quad (eq. 7)$$

$$192 \quad AMAPE = \frac{1}{n} \sum_{t=1}^n \left(\frac{|\hat{z}_t - z_t|}{\frac{1}{n} \sum_{t=1}^n z_t} \right) * 100\% \quad (eq. 8)$$

193

194 where t represents the time and n is the sample size for forecasts; \hat{z}_t is the forecast at t from any mentioned
195 model and z_t is the actual value at t . The RMSE statistic depends on the scale of the variables and measures
196 the absolute errors. The AMPAE statistic measures the relative errors. The smaller the RMSE and AMAPE the
197 better the accuracy of the model.

198

199 However, the model could give good results in the accuracy measurements for three-months-ahead, but poor
200 results for one-year-ahead, for instance, which means the impact of the model uncertainty on forecasts needs
201 to be measured (Chatfield, 2000). In this study, a measure was used based on the variance of forecast errors
202 (difference between the actual and forecast value) to quantify this uncertainty. The smaller the variance the less
203 uncertain the model or the more accurate the forecast results. The variance of error for sample size n for forecasts
204 is defined as:

205

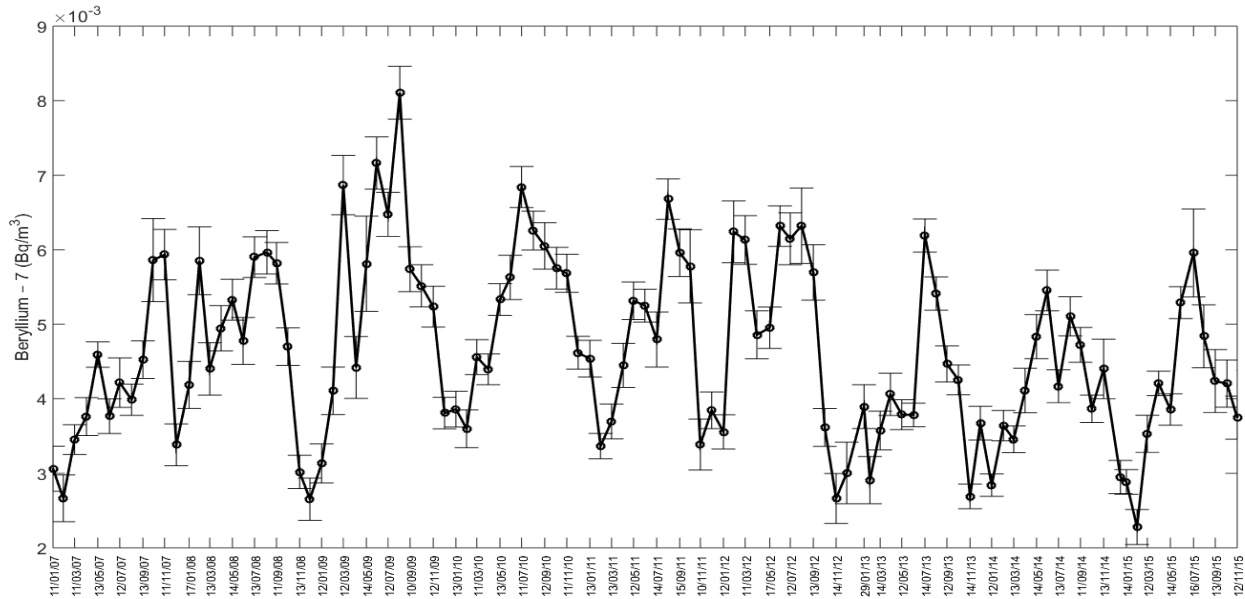
206

$$207 \quad \sigma_{\varepsilon}^2 = \frac{1}{n} \sum_{t=1}^n \left(\left[\frac{|\hat{z}_t - z_t|}{\frac{1}{n} \sum_{t=1}^n z_t} \right] - \frac{1}{n} \sum_{t=1}^n \left(\frac{|\hat{z}_t - z_t|}{\frac{1}{n} \sum_{t=1}^n z_t} \right) \right)^2 \quad (eq. 9)$$

208

209 3. Results and discussion

210 Figure 1 shows the evolution of the actual ^7Be air concentrations and its measurement uncertainty during the
 211 entire study period from 2007 to 2015. A seasonal pattern with a sinusoidal trend can be clearly seen.

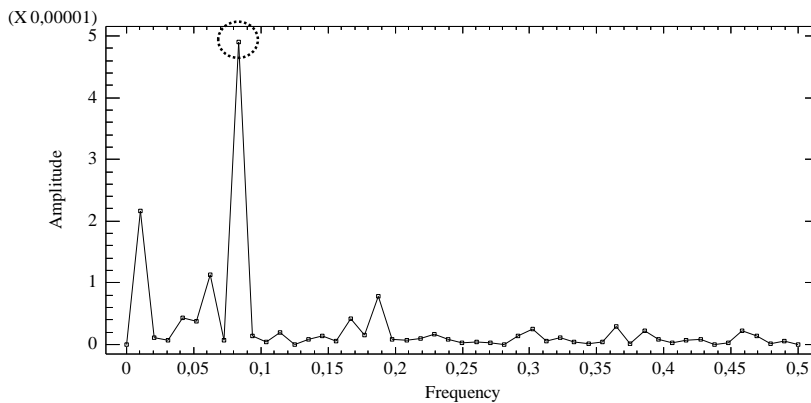


212 Fig 1. Temporal evolution of ^7Be air concentration over the period 2007-2015.

213 The steps involved in developing a SARIMA model are applied to different data ranges of historical data in
 214 order to identify and validate the number of periods which best fit actual ^7Be data.

215
 216 First of all, results in Table 1 show the identification of a SARIMA model for each data range proposed, which
 217 were between two and eight years of historical data, considering 2007 as the initial year.

218 In the identification and estimation step, the periodogram analysis was applied to all the time series considered
 219 All these results identified a relevant peak of a period of 12 months (annual periodicity) ($s = 12$). For instance,
 220 Figure 2 shows the periodogram plot for the ^7Be time series over period 2007-2014. In this periodogram, one
 221 relevant peak is observed, corresponding to a cyclical period of 12 months ($1/0.083333$), which indicates an
 222 annual periodicity.



223
 224
 225
 226
 227
 228
 229
 230
 231 Fig 2. Periodogram of the ^7Be time series over the period 2007-2014

232 After differencing the time series and trying several combinations for parameters p , q , P and Q , based on the
 233 shape of the ACF and PACF, the best and most parsimonious model was selected, considering the minimum

234 AMAPE and RMSE for the forecasting data as accuracy measures of the predictive power. Tables 1 reports the
235 results of the parameters p, d, q, P, D and Q identified for each selected model over the time period specified.

236 In the validation step, the t-ratio test, the Kolmogorov-Smirnov test and the Q^* Ljung-Box test introduced in
237 Section 2.3 were applied to validate the adequacy of the identified models for each time period. Tables 1 show
238 that, since they pass the above tests (p-values for *t-ratio test* are less than 0.05 and p-values for *K-S* and *Q**
239 *tests* are greater than 0.05) all the models selected to explain ^7Be air concentrations in a specific time period
240 could be used to make forecasts.

241
242 The training data used for model fitting in the forecasting step was the data from the time period specified in
243 Table 1, and the test sample used to evaluate the established model was the data of the year following the time
244 period analyzed.

245 Figures 4-5 show the RMSE, AMAPE for the different models proposed. Note that RMSE and AMAPE values
246 were calculated considering the sample sizes for out-of-sample forecasts of 1,3,6,9, and 12 months. As can be
247 observed, in general, the RMSE value for 1 month is very different to that of more than 1 month, suggesting
248 that predictions for one month period are uncertain. The selection model criteria are thus based on forecasts of
249 at least three months.

250 The models estimated with only a few years of historical data have higher values for the accuracy measurements
251 in the forecasting sample sizes proposed (Figures 4-5), which means these models have a high degree of
252 uncertainty and are therefore not useful for predicting ^7Be concentrations. As an exception, the model proposed
253 with a time window of three years (2007-2009) provides good results in the RMSE and AMAPE coefficients
254 for a forecasting sample of more than three months. However, the accuracy measurements for three-months-
255 ahead are somewhat higher, indicating that the forecasting errors are not constant and the model is uncertain
256 for short-term forecasting.

257 Figures 4-5 show that the $\text{SARIMA}(0,1,1)\times(1,1,3)_{12}$ model provides good results for the RMSE and AMAPE
258 accuracy measurements in a time window of seven (2007-2013) or eight (2007-2014) years. However, a time
259 series with an 8-year time window appears to be better, because the measurement based on the variance of the
260 forecast errors defined in eq. 9, is lower, $\sigma_{\varepsilon}^2 = 0.0067$ (Table 1), indicating that the model is less uncertain and
261 the errors are more constant and stable across a one-year-ahead forecast. This result shows it is important to
262 control the quality of the forecasting data. Note that the errors are minimal with a forecast window of six
263 months.

264 In order to confirm these results and identify the time window that best fits ^7Be air concentrations, the analysis
265 was repeated remaining the out-of sample fixed to the year 2015. Results are showed in Table 2.

266 The steps applied to identify and validate the best model in each period of time proposed in Table 2 are the
267 same as the steps followed and explained above for Table 1.

268 Again, the RMSE, AMAPE and the low value in σ_{ε}^2 (Figure 4-5 and Table 2 respectively) suggest that the
269 model with 8 years of historical data (2007-2014) is the most suitable for monitoring and forecasting ^7Be data.

270

271

272

273

274

275

276

277

278

279

280

281

282

283

284

285

286

287

288

289

290

291

292

Model Identification and Estimation		Model Validation			Model Forecasting
Period	Parameters	t-ratio statistic (p-value)	K-S statistic (p-value)	Q* statistic (p-value) m=n° of lags	σ_ε^2
2007-2008	(0,1,0)(1,0,1) ₁₂	Φ_1 6.74 (0.000001) θ_1 9.45 (<0.000001)	0.11073 (0.6571)	17.541 (0.0632) m=12	0.0493
2007-2009	(0,1,1)(1,1,2) ₁₂	θ_1 3.20 (0.004637) Φ_1 -4.03 (0.000701) θ_1 -2.28 (0.033760) θ_2 4.94 (0.000090)	0.092656 (0.8756)	10.468 (0.2337) m=12	0.0143
2007-2010	(0,1,1)(0,1,2) ₁₂	θ_1 3.50 (0.001381) θ_1 13.16 (<0.000001) θ_2 -7.06 (<0.000001)	0.06604 (0.9623)	29.061 (0.1125) m=24	0.0236
2007-2011	(0,1,1)(2,1,2) ₁₂	θ_1 7.18 (<0.000001) Φ_1 -4.84 (0.000017) Φ_2 -18.06 (<0.000001) θ_1 7.13 (<0.000001) θ_2 -3.55 (0.000951)	0.12184 (0.078)	18.998 (0.9549) m=36	0.0224
2007-2012	(0,1,1)(2,1,2) ₁₂	θ_1 8.71 (<0.000001) Φ_1 -5.14 (0.000004) Φ_2 -14.91 (<0.000001) θ_1 10.30 (<0.000001) θ_2 -5.08 (0.000005)	0.08602 (0.3415)	39.543 (0.622) m=48	0.0599
2007-2013	(0,1,1)(1,1,3) ₁₂	θ_1 7.08 (<0.000001) Φ_1 -6.84 (<0.000001) θ_1 6.59 (<0.000001) θ_2 14.74 (<0.000001) θ_3 -12.12 (<0.000001)	0.074491 (0.426)	48.092 (0.2742) m=48	0.0172
2007-2014	(0,1,1)(1,1,3) ₁₂	θ_1 8.04 (<0.000001) Φ_1 -9.49 (<0.000001) θ_1 8.08 (<0.000001) θ_2 19.50 (<0.000001) θ_3 -13.70 (<0.000001)	0.079983 (0.2119)	47.809 (0.2837) m=48	0.0067

Table 1. SARIMA models proposed for different time window data.

293

294

295

296
297
298
299
300
301
302
303
304
305
306
307
308
309
310
311
312
313
314

Model Identification and Estimation		Model Validation			Model Forecasting	
Period	Parameters		t-ratio statistic (p-value)	K-S statistic (p-value)	Q* statistic (p-value) m=n ^o of lags	σ_{ε}^2
2013-2014	(1,1,0)(1,0,0) ₁₂	ϕ_1	4.02 (0.000609)	0.17806	9.2619	0.1290
		Φ_1	-30.87 (<0.000001)	(0.05674)	(0.5074) m=12	
2012-2014	(0,1,1)(0,1,2) ₁₂	θ_1	6.13 (0.000005)	0.088324	10.972	0.0219
		θ_1	8.90 (<0.000001)	(0.913)	(0.277) m=12	
2011-2014	(0,1,1)(0,1,3) ₁₂	θ_1	7.80 (<0.000001)	0.10949	27.277	0.0363
		θ_1	15.48 (<0.000001)	(0.3577)	(0.1276) m=24	
2010-2014	(0,1,1)(2,1,2) ₁₂	θ_1	5.36 (0.000003)	0.093043	28.889	0.0359
		Φ_1	-9.53 (<0.000001)	(0.3909)	(0.575) m=36	
2009-2014	(0,1,1)(2,1,2) ₁₂	θ_1	7.35 (<0.000001)	0.068811	45.291	0.0167
		θ_2	-4.22 (0.000124)	(0.696)	(0.3766) m=48	
2008-2014	(0,1,1)(3,1,2) ₁₂	θ_1	11.09 (<0.000001)	0.069582	34.671	0.0146
		Φ_1	-2.54 (0.013958)	(0.5373)	(0.7816) m=48	
2007-2014	(0,1,1)(1,1,3) ₁₂	Φ_2	-7.54 (<0.000001)	0.079983	47.809	0.0067
		θ_1	13.04 (<0.000001)	(0.2119)	(0.2837) m=48	
		θ_2	-6.67 (<0.000001)			
		θ_1	9.79 (<0.000001)			
		Φ_1	-4.29 (0.000059)			
		Φ_2	-9.99 (<0.000001)			
		Φ_3	-5.42 (0.000001)			
		θ_1	13.77 (<0.000001)			
		θ_2	-6.92 (<0.000001)			
		θ_1	8.04 (<0.000001)			
		Φ_1	-9.49 (<0.000001)			
		θ_1	8.08 (<0.000001)			
		θ_2	19.50 (<0.000001)			
		θ_3	-13.70 (<0.000001)			

315

Table 2. SARIMA models proposed for different time window data with common out-of-sample.

316
317
318
319
320
321
322
323
324
325
326
327
328
329
330
331
332
333
334

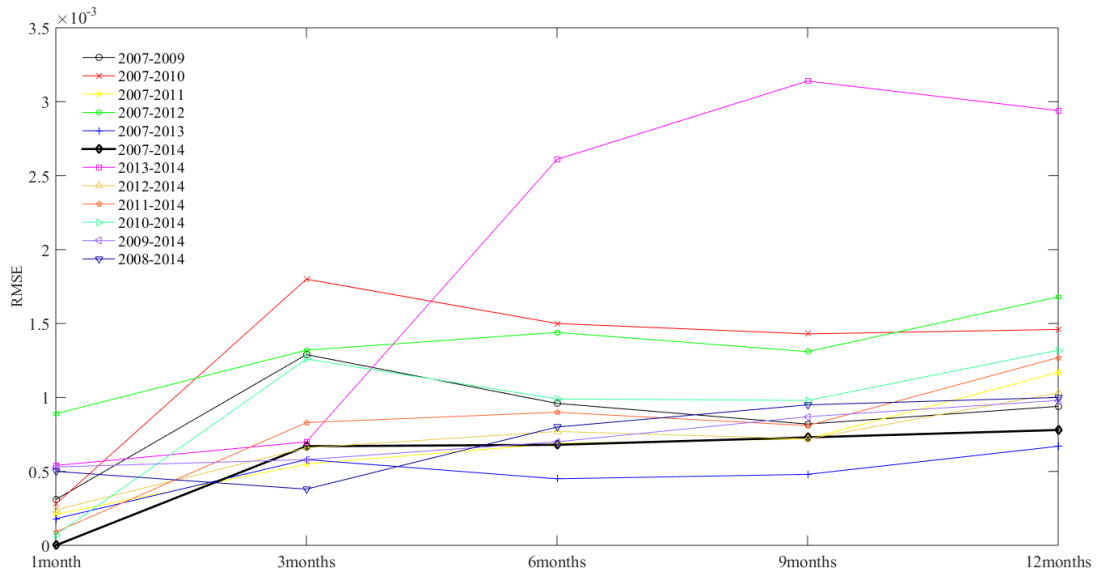
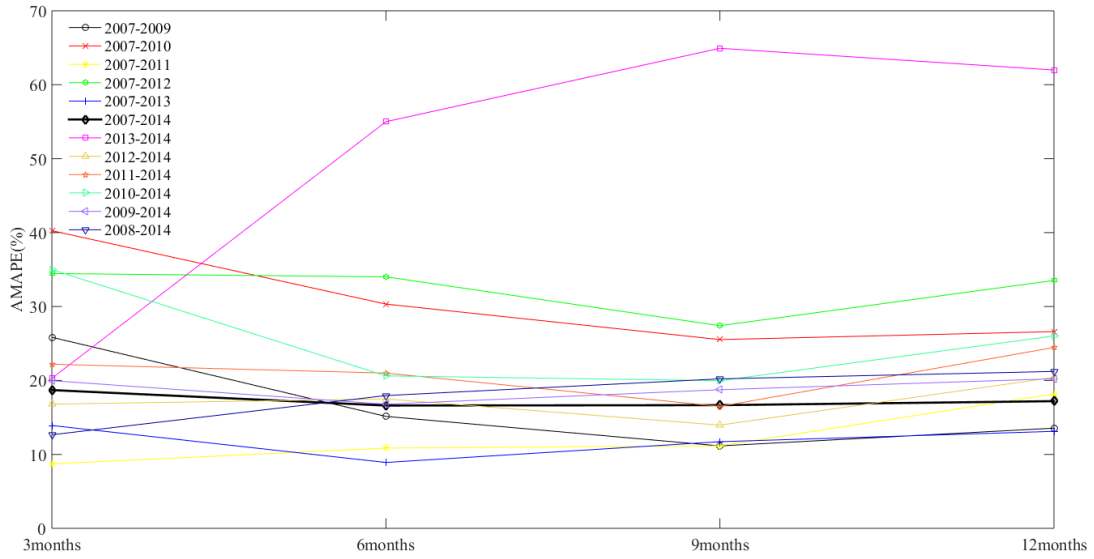


Fig 4. RMSE (eq. 7) for models evaluated in table 1 and 2.

335
336
337
338
339
340
341
342
343
344
345
346
347
348
349
350
351



352
353

Fig 5. AMAPE (Eq. 8) for models evaluated in Tables 1 and 2.

354 The estimated and validated SARIMA(0,1,1)x(1,1,3)₁₂ model proposed for a time window of eight years
355 (2007-2014) is:

$$356 \quad \Phi_1(B^{12})(1 - B)^1(1 - B^{12})^1 z_t = \theta_1(B)\theta_3(B^{12})a_t \quad (eq. 10)$$

357
358

The coefficients are estimated by a maximum likelihood function, obtaining the following values:

$$359 \quad \theta_1 = 0.665$$

$$360 \quad \Phi_1 = -0.814$$

$$361 \quad \theta_1 = 0.555$$

$$362 \quad \theta_2 = 0.932$$

$$363 \quad \theta_3 = -0.687$$

364

365 Considering Equations 2 to 5 and the estimated parameters above, Equation 10 can be expressed as follows:
366 $(1 + 0.814B^{12})(1 - B)(1 - B^{12})z_t = (1 - 0.665B)(1 - 0.555B^{12} - 0.932B^{24} + 0.687B^{36})a_t$ (eq. 11)

367 where $a_t \approx WN(0, 6.6E - 07)$ and B is the lag operator.

368 According to Bas et al. (2016), ⁷Be concentration variability can be decomposed into terms of three main
369 components: 1) trend-cycle, 2) seasonal and 3) irregular variations. Solar activity is a cosmogenic factor with
370 a high influence on the trend-cycle component of ⁷Be variability. Solar radiation, temperature and relative
371 humidity are influential factors in seasonal ⁷Be variations and, finally, precipitations and wind speed influence
372 the irregular part of the ⁷Be time series decomposition.

373 Considering the results obtained in Bas et al. (2016) and the model proposed in this paper (Eq. 11), the following
374 relation between the SARIMA parameters and the atmospheric factors could be interpreted.

375 In the model proposed, the parameter p is zero; this result means that no significant influence of the ⁷Be for the
376 previous months of the same year was observed on the ⁷Be for the forecasting month, which means that the
377 time series has no inertia.

378 The coefficient $(1 + 0.814B^{12})$ is associated with the parameter $P=I$, which determines the influence of the
379 months of previous years on the forecasting month; for instance, the forecasting value for ⁷Be activity in January

380 2015 is influenced by the ${}^7\text{Be}$ activity observed in January 2014. The dependence observed between the
381 seasonal observations could be influenced by solar radiation, temperature and relative humidity, which are
382 regular atmospheric variables that affect seasonal ${}^7\text{Be}$ variations (Bas et al., 2016).

383 The coefficient $(1 - B)$ is associated with the parameter $d=1$, which recognize the presence of a trend in the
384 time series. This trend could be affected by solar activity considering the results of Bas et al. (2016). The model
385 proposed is able to detect a trend influenced by a part of the solar cycle, but is unable to model the cycle
386 component due to solar activity because the evaluated period is too short.

387 The parameter $D=1$ recognize the presence of an annual seasonality and is associated with the coefficient
388 $(1 - B^{12})$ in the model. This coefficient eliminates the visual part of the seasonality in order to capture the real
389 dependencies between the months in different years.

390 The coefficient $(1 - 0.665B)$ is associated with the parameter $q=1$. This coefficient identifies the influence of
391 external factors, which affected the previous month, on the forecasting month. According to the results of Bas
392 et al. (2006), these external factors could be precipitation and wind speed, among others, due to their irregular
393 and random behavior. This result means that the ${}^7\text{Be}$ activity obtained in the forecasting months through the
394 model is affected by the irregular factors that happened in the previous month.

395 Finally, the coefficient $(1 - 0.555B^{12} - 0.932B^{24} + 0.687B^{36})$ is associated with the parameter $Q=3$ and
396 also captures the influence of random factors such as precipitation and wind speed, which affected months of
397 the previous three years, on the forecasting month. In general, this parameter captures the long-term influence
398 of external factors on the forecasting month.

399 Figure 6 shows the comparison between measured and forecast values using a $\text{SARIMA}(0,1,1)\times(1,1,3)_{12}$ in a
400 training sample 2007-2014.

401
402
403
404
405
406
407
408
409
410
411
412
413
414
415
416
417
418
419
420

421
 422
 423
 424
 425
 426
 427
 428
 429
 430
 431
 432
 433
 434
 435
 436
 437
 438
 439
 440
 441
 442
 443
 444
 445
 446
 447
 448
 449
 450
 451
 452
 453
 454
 455
 456
 457
 458
 459
 460
 461
 462
 463
 464
 465
 466
 467
 468
 469
 470
 471

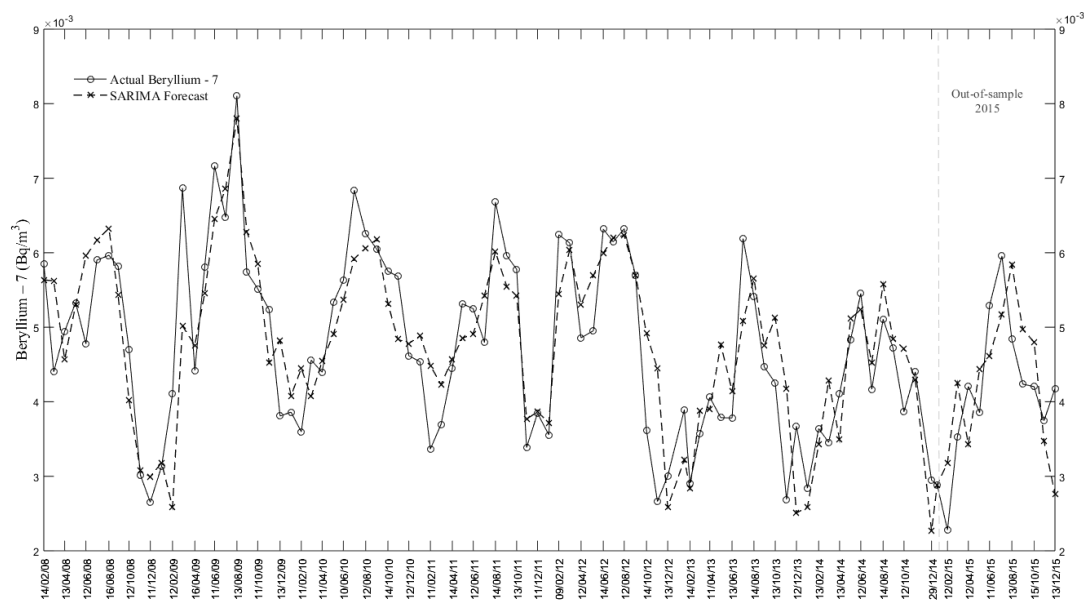


Fig 6. Comparison between measured and forecast (SARIMA) power

4. Conclusions

A Seasonal Autoregressive Integrated Moving Average (SARIMA) model was proposed in different year ranges to forecast ^7Be air concentrations in Valencia, in particular a $\text{SARIMA}(p, d, q)(P, D, Q)_s$. The forecasting results for the different models were compared and analyzed for the subsequent 12 months by out-of-sample tests.

The results show that the best time series models are based on a time window of at least eight years of data when forecasting ^7Be concentrations. Considering the forecasting power measured by the RMSE and AMAPE accuracy coefficients and the impact of the model uncertainty measured by the variance of the errors, a $\text{SARIMA}(0,1,1)\times(1,1,3)_{12}$ model was proposed to best fit ^7Be concentration data for a time window of eight years (2007-2014). The prediction results for the out-of-sample year are appropriate and the errors observed are constant, with a minimum uncertainty of $\sigma_\varepsilon^2 = 0.0067$. The results show also that the optimal forecasting time range is six months, since the errors are higher for longer prediction periods.

The time series models proposed in this paper have the advantage of not requiring any forecast meteorological parameters to develop the model, as is required for a Multiple Linear Regression (MLR) model. In this case, ^7Be forecasting can thus be adopted as a target value in analyzing deviations that could imply important atmospheric changes. The forecasting values obtained with SARIMA models do not explicitly capture an anomaly in specific atmospheric variables, which is the advantage of the MLR model. However, the SARIMA model can detect that a deviation occurred and was produced by an atmospheric factor. The SARIMA models combined with the influence of exogenous factors could cope with this problem and would be an interesting subject for future research. Despite this limitation, the model proposed in this study, in addition to the results of Bas et al. (2016), point to an interesting relationship between the model and the atmospheric parameters.

The availability of further data measurements will make it possible to adjust a time series with a wider time window period to submit the minimum period of years that best fit ^7Be air concentrations to a further analysis. For instance, the availability of more complete solar cycles could provide enough information to explicitly model the trend-cycle component. With regard to the application, one could envisage that it will be possible to develop the proposed forecasting models not only for ^7Be air concentrations, but also for monitoring and forecasting a range of different radionuclides.

472 **5. Acknowledgements**

473 This study has been supported partially by the REM program of the Nuclear Safety Council of Spain
474 (SRA/2071/2015/227.06).

475

476 **Bibliography**

477 Alwan, L.C., Roberts, H.V.1988. Time series modelling for statistical process control. *Journal of Business and Economic Statistics*, 6,
478 87-95.

479 Azahra, M., López-Peñalver, J.J., Camacho García, C., González-Gómez, C., El Bardouni T., Boukhal, H. 2004a. Atmospheric
480 concentrations of ⁷Be and ²¹⁰Pb in Granada, Spain. *Journal of Radioanalytical and Nuclear Chemistry*, 261,401-405.

481 Azahra, M., González-Gómez, C., López-Peñalver, J.J., El Bardouni, T., Camacho García, A., Boukhal, H., El Moussaoui, F., Chakir,
482 E., Erradi, L., Kamili, A., Sekaki, A. 2004b.The seasonal variations of ⁷Be and ²¹⁰Pbconcentrations in air. *Radiation Physics and*
483 *Chemistry*, 71, 789–790.

484 Bas, M.C., Ortiz, J., Ballesteros, L., Martorell, S. 2016. Analysis of the influence of solar activity and atmospheric factors on ⁷Be air
485 concentration by seasonal-trend decomposition. *Atmospheric Environment*, 145, 147-157.

486 Baeza, A., Del Río, L.M., Jiménez, A., Miró, C., Paniagua, J.M., Rufo, M., 1996. Analysis of the temporal evolution of atmospheric
487 ⁷Be as a vector of the behavior of other radionuclides in the atmosphere. *Journal of Radioanalytical and Nuclear Chemistry*, 207, 331-
488 344.

489 Box, G.E.P., Jenkins, G.M.1976. *Time series analysis: forecasting and control*. San Francisco: Holden Day.

490 Bruninx, E. 1961. High-energy nuclear reaction cross-sections. III Report CERN 64-17, Geneva, Switzerland.

491 Chatfield, C. 2000. *Time-Series Forecasting*. London, U.K.: Chapman & Hall/CRC.

492 Dueñas, C., Fernández, M.C., Cabello, M., Gordo, E., Liger, E., Cañete, S., Pérez, M. 2015.Study of the cosmogenic factors influence
493 on temporal variation of ⁷Be air concentration during the 23rd solar cycle in Málaga. *Journal of Radioanalytical and Nuclear Chemistry*,
494 303, 2151-2158.

495 Dueñas, C., Fernández, M.C., Liger, E., Carretero, J. 1999. Gross alpha, gross beta activities and ⁷Be concentrations in surface air:
496 analysis of their variations and prediction model. *Atmospheric Environment*, 33, 3705-3715.

497 Feely, H.W., Larsen, R.J., Sanderson, C.G. 1989. Factors that cause seasonal variations in Beryllium-7 concentrations in surface air.
498 *Journal of Environmental Radioactivity*, 9, 223-249.

499 Harris, T.J., Ross, W.H. 1991. Statistical process control procedures for correlated observations. *Canadian Journal of Chemical*
500 *Engineering*, 69, 48–57.

501 Hötzl, H., Rosner, G., Winkler, R., 1991. Correlation of ⁷Be concentrations in surface air and precipitation with the solar cycle.
502 *Naturwissenschaften*, 78, 215-217.

503 Ioannidou, A., Papastefanou, C., 1994. Atmospheric Beryllium-7 concentrations and sun spots. *Nuclear Geophysics*, 8, 539-543.

504 Kotsopoulou, E., Ioannidou A., 2012. ⁷Be atmospheric concentration at mid latitudes (40°N) during a year of solar minimum. In
505 *Proceedings EPJ Web of Conferences*. Vol 24. <http://dx.doi.org/10.1051/epiconf/20122405005>.

506 Lal, D., Malhotra, P.K., Peters, B., 1958. On the production of radioisotopes in the atmosphere by cosmic radiation and their application
507 to meteorology. *Journal of Atmospheric and Solar-Terrestrial Physics*, 12, 306-328.

508 O'Brien, K., 1979. Secular variations in the production of cosmogenic isotopes in the earth's atmosphere. *Journal of Geophysical*
509 *Research*, 84, 423-431.

510 Peña, D. (2010). *Análisis de series temporales*. Madrid: Alianza Editorial.

511 Piñero-García, F., Ferro-García, M.A., Azahra, M. 2012. ⁷Be behaviour in the atmosphere of the city of Granada January 2005 to
512 December 2009. *Atmospheric Environment*, 47, 84-91.

513 Piñero-García, F., Ferro-García, M.A. 2013. Evolution and solar modulation of ⁷Be during the solar cycle 23. *Journal of Radioanalytical*
514 *and Nuclear Chemistry*, 296, 1193-1204.

- 515 Schuster, A.1898. On the investigation of hidden periodicities with application to a supposed 26 day period of meteorological
516 phenomena, *Terrestrial Magnetism*, 3, 13-41.
- 517 Shine, D.W., Lee, J.H., 2000. Consistency of the maximum likelihood estimators for nonstationary ARIMA regressions with time
518 trends. *Journal of Statistical Planning and Inference*, 87, 55-68.
- 519 Shumway, R.H., Stoffer, D.S., 2006. *Time series analysis and its applications: With R Examples*. Springer Texts in Statistics. New
520 York: Springer-Verlag.
- 521 Tsay, R. S. 2005. *Analysis of Financial Time Series*, 2nd ed. New York: Wiley.
- 522 Vogt, S., Herzog, G.F., Reedy, R.C., 1990. Cosmogenic nuclides in extraterrestrial materials. *Reviews of Geophysics*, 28, 253-275.
- 523 Wardell, D.G., Moskowitz, H., Plante, R.D.1994. Run length distributions of special-cause control charts for correlated processes.
524 *Technometrics*, 36, 3-17.
- 525 Wu, L., Shahidehpour, M. 2010. A Hybrid Model for Day-Ahead Price Forecasting. *IEEE Transactions on power systems*, 25, 1519-
526 1530.